Steric antisense inhibition of AMPA receptor Q/R editing reveals tight coupling to intronic editing sites and splicing

Article (Published Version)

Published online 20 November 2012 *Nucleic Acids Research, 2013, Vol. 41, No. 2* ***1113–1123***
doi:10.1093/nar/gks1044

Steric antisense inhibition of AMPA receptor Q/R editing reveals tight coupling to intronic editing sites and splicing

Andrew C. Penn*, Ales Balik and Ingo H. Greger*

Neurobiology Division, MRC Laboratory of Molecular Biology, CB2 0QH Cambridge, UK

Received August 11, 2012; Revised October 3, 2012; Accepted October 8, 2012

ABSTRACT

Adenosine-to-Inosine (A-to-I) RNA editing is a post-transcriptional mechanism, evolved to diversify the transcriptome in metazoa. In addition to wide-spread editing in non-coding regions protein recoding by RNA editing allows for fine tuning of protein function. Functional consequences are only known for some editing sites and the combinatorial effect between multiple sites (functional epistasis) is currently unclear. Similarly, the interplay between RNA editing and splicing, which impacts on post-transcriptional gene regulation, has not been resolved. Here, we describe a versatile antisense approach, which will aid resolving these open questions. We have developed and characterized morpholino oligos targeting the most efficiently edited site—the AMPA receptor GluA2 Q/R site. We show that inhibition of editing closely correlates with intronic editing efficiency, which is linked to splicing efficiency. In addition to providing a versatile tool our data underscore the unique efficiency of a physiologically pivotal editing site.

INTRODUCTION

Adenosine-to-Inosine (A-to-I) RNA editing, the post-transcriptional conversion of single nucleotides in pre-mRNA, is a unique mechanism for protein diversification particularly in the nervous system (1–3). This process requires RNA secondary structures within primary mRNA transcripts that are recognized by adenosine deaminases [adenosine deaminases acting on RNA (ADARs)], which catalyze the conversion of adenosine to inosine. During translation of edited coding sequences, inosine is recognized as guanosine thus resulting in a change to the RNA codon and often the protein sequence (4,5). ADARs are essential, their deletion results in premature death in vertebrates and to severe nervous system dysfunction in invertebrates (2). In addition to fine-tuning function of central signaling molecules RNA editing abundantly targets non-transcribed regions, particularly in vertebrates and thereby regulates RNA metabolism (1).

The first A-to-I site to be described was the Q/R site in AMPA-type glutamate receptors (AMPARs) (6): cation channels mediating the bulk of fast excitatory neurotransmission in vertebrate brains (7). This editing site locates to the channel pore where it determines ion flux and channel assembly (6,8). Edited varieties render the channel Ca^{2+} impermeable, and by disfavoring assembly of edited homotetrameric GluA2 the formation of AMPAR heteromers is enabled. GluA2 Q/R editing is essential for survival, the site is edited to >99% (6). Reduced GluA2 Q/R editing in gene-targeted mice results in severe seizures and premature death, which is linked to altered Ca^{2+} permeability through AMPARs (9,10). The Q/R site is exclusively edited by the editase *Adar2*; deletion of the *Adar2* locus resembles the severe phenotype of editing-deficient *Gria2* alleles, and is rescued by expression of a Q/R-edited *Gria2* allele (in the $Adar2^{-/-}$ background) (11). Moreover, underediting of the Q/R site is associated with a variety of diseases in humans, such as epilepsy ischemia and amyolateral sclerosis (ALS) (2,12,13). ALS has been studied in some detail, where it appears that reduced expression of *ADAR2* are linked to reduced Q/R editing resulting in motor neuron degeneration (13). Together, these findings highlight the unique nature of the GluA2 Q/R site, with efficient editing being pivotal to survival of the organism. The question of why this critical position 'relies' on editing, rather than being hardwired into the genome, remains a mystery (14).

*To whom correspondence should be addressed. Tel: +44 1223 402 173; Fax: +44 1223 402 310; Email: ig@mrc-lmb.cam.ac.uk
Correspondence may also be addressed to Andrew Penn. Tel: +33 5 57 57 40 80. Fax: +33 5 57 57 40 82; Email: andrew.penn@u-bordeaux2.fr
Present addresses:
Andrew C. Penn, Interdisciplinary Institute for Neuroscience, Univ. de Bordeaux, UMR 5297, F-33000 Bordeaux, France; CNRS, Interdisciplinary Institute for Neuroscience, UMR 5297, F-33000 Bordeaux, France.
Ales Balik, Institute of Physiology, Academy of Sciences of the Czech Republic v.v.i., Videnska 1083, 142 20 Prague 4, Czech Republic.

High-throughput approaches increasingly demonstrate a prominent role for A-to-I editing in development, metabolism and in disease (15). Contrasting with the rapid pace of these technical developments is a good understanding of the biology of individual editing sites. Antisense probes provide unique versatility to interfere with RNA-based processes including splicing and translation, where this approach has provided key insights. In the context of editing, a steric block antisense oligonucleotide (oligo) could be designed to hybridize to the editing site complementary sequence (ECS) and/or double stranded RNA binding sites of ADARs. As the secondary structure is essential for Adar binding, strand invasion and hybridization of the antisense oligo would inhibit A-to-I editing (Figure 2). This substrate-targeted approach could permit site-specific manipulation of endogenous editing sites. A widely used antisense oligo for steric antisense applications is the morpholino oligo. Morpholinos have been used extensively to modify pre-mRNA splicing, block mRNA translation and inhibit miRNA maturation or activity (16,17). Importantly given the duplex structure of the Q/R editing substrate, potent antisense activity of morpholinos has been demonstrated on highly structured RNA targets (18–20).

Here, we first provide an in-depth characterization and evolutionary relationships of the GluA2 AMPAR Q/R editing substrate. We go on to describe experiments that provide a proof-of-principle for substrate-targeted competitive inhibition via antisense probes. We then use the antisense strategy to characterize the link between Q/R editing and intron 11 splicing and demonstrate the remarkable resilience of the GluA2 Q/R site. This approach will facilitate an in-depth characterization of individual metazoan A-to-I RNA editing sites.

MATERIALS AND METHODS

Bioinformatics

The imperfect inverted repeat containing the Q/R site was identified from the rat *Gria2* gene sequence (exons 11–12) using the EINVERTED application of a locally installed European Molecular Biology Open Software Suite (EMBOSS) [Version 6.0.1; (21) interfaced with Jemboss Graphical User Interface (GUI) (Version 1.5)] (22). The imperfect inverted repeat of rat along with some flanking sequence was used as a Basic Local Alignment Search Tool (BLAST) or BLAST-Like Alignment Tool (BLAT) search query to indentify homologs from the online Ensembl and Pre-Ensembl vertebrate assemblies (23–25). Likewise, shark sequence was retrieved from the whole genome shotgun sequence database on the Institute of Molecular and Cell Biology server (26). The sequence coordinates and associated information are documented in Supplementary Table S1. Sequences were aligned using Multiple Alignment based on Fast Fourier Transform (MAFFT) by iterative refinement with pairwise alignment information [L-INS-i; Version 6.903; (27)]. Sequence similarity was calculated and data output from the PLOTCON application in EMBOSS using the EDNA scoring matrix and a window size of 1. The γ-centroid consensus structure was predicted from the alignment using CentroidAlifold with a default inference engine [Version 0.0.9; (28)]. The common structure was superimposed onto the rat GluA2 pre-mRNA sequence and visualized with Visualization Applet for RNA (VARNA) [Version 3.8; (29)]. The posteriors were used to plot the probabilities of base pairs shown in the consensus structure.

Cell culture

HEK-293T, HeLa and SH-SY5Y cells were cultured in Dulbecco's modified Eagle's medium (DMEM) (containing glutamax 1; GIBCO) supplemented with 10% heat-inactivated (56° C, 30 min) fetal bovine serum (FBS) and penicillin/streptamycin (Pen/Strep). MIN-6 cells were cultured in DMEM (GIBCO) containing 10% heat-inactivated FBS and (in mM): dextrose (25), L-Glutamine (1), β-mercaptoethanol (0.0715) and Pen/Strep. Plasmid DNA constructs were transfected into Hek 293T and HeLa cells using Effectene (Qiagen) and Lipofectamine 2000 (Invitrogen), respectively. Morpholinos were delivered into all cell lines (except MIN-6) using Endo-Porter (Gene Tools) (30). Transfections into MIN-6 cells were by electroporation using solution kit R and program T-027 (Amaxa).

Molecular biology

Morpholino 25-mer oligos with a 3′-carboxyfluorescein end modification were ordered from Genetools, LLC (www.gene-tools.com) Morpholino sequences are detailed in the Supplementary Table S2. The standard negative control morpholino (control) is expected to not cause effect as it only shows complementarity to an aberrant 5′ splice site created by a point mutation in the second intron of the β-globin gene (IVS2705) in a subset of human β-thalassemia patients (31). DNA and RNA were extracted from cells and tissues by the acid guanidinium thiocyanate-phenol-chloroform procedure, using Trizol according to the manufacturers' instructions (15596, Invitrogen). For RNA, the pellet was resuspended in buffer (in mM): Tris-Cl (40), NaCl (10), $CaCl_2$ (1), $MgCl_2$ (6) supplemented with 0.5 U/μl human placental ribonuclease inhibitor (N2111, Promega) and 0.1 U/μl RNase-free DNase I (Roche). DNA digestion proceeded at 37° C for ~0.5 h. Samples were diluted to 0.5 ml with Rnase-free water (Ambion) and RNA was repurified by mixing with one volume of 5:1 acid phenol:chloroform (pH 4.3) and spinning down at 10 000g for 5 min at room temperature in a bench top centrifuge. The aqueous supernatant was transferred to a new microcentrifuge tube and residual phenol was removed by mixing with one volume of chloroform and spinning down as before. RNA was precipitated with 20 μg glycogen, 0.3 M sodium acetate (pH 5.2) and one volume of isopropanol at room temperature and pelleted at 10 000g for 10 min at 4° C or room temperature. The RNA pellet was washed with 75% ethanol, air-dried and resuspended in Rnase-free water (Ambion). Ribosomal RNA integrity was assessed by native agarose gel electrophoresis and cDNA synthesis was carried out

using random hexamers (Invitrogen) and Avian Myeoloblastosis Virus reverse transcriptase according to the Gübler and Hoffman procedure in the manufacturers instructions (SuperRT, HT Biotechnology). PCR amplicons from cDNA templates were subjected to restriction digests with either BbvI (GCAGC) or TauI (GCGGC), or products were sequenced with the Sanger method and the relative peaks of nucleotides at the position of the editing sites were quantified using PeakPicker (32) or BioEdit software (http://www.mbio.ncsu.edu/bioedit/bioedit.html).

For experiments with reporter constructs, PCR amplification of the minigene transcript was achieved from the cDNA of cell RNA extract. In addition to the use of DNase I digestion of RNA samples, contamination of plasmid DNA was minimized by amplification using primers spanning efficiently spliced introns native to the pCI-neo and pET01 vectors, which expressed the GluA2 Q/R and R/G site minigenes, respectively. The Q/R site minigene was a cloned BglII–XbaI fragment of the rat *Gria2* gene encompassing the 3′ half of exon 11 and the 5′-end of intron 11–12. The R/G site minigene was a cloned fragment of the mouse *Gria2* gene encompassing exons 13–16.

RESULTS

Properties of the Q/R substrate

The Q/R site is located near the end of exon 11 of the *Gria2* locus (Figure 1A). Here, it exists within an imperfect inverted repeat, which extends into intron 11–12 and forms a complex pre-mRNA secondary structure subject to deamination by Adar2 (Figure 1A: inset) (33). To investigate attributes of the Q/R site substrate underlying its efficient editing we used a bioinformatics approach to examine genetic variations that are permissive for editing *in situ*. For this, we focused on genome sequencing projects from 50 vertebrate species with diploid genomes, including 1 cartilaginous fish (*Chondrichtyes*), 1 amphibian (*Amphibia*), 2 turtles (*Anapsida*), 1 scaled reptile and 5 birds (*Diapsida*), 1 egg laying mammal (*Prototheria*), 2 marsupials (*Metatheria*) and 37 placental mammals (*Eutheria*) (Supplementary Table S1). Polyploidy in bony, ray-finned fish (*Actinopterygii*) had introduced a second GluA2 subunit genomically encoding an arginine at the Q/R site position (gria2β), which could reduce evolutionary pressure to maintain high A-to-I editing efficiency in the primary subunit (gria2α) and so were not included. Aligned DNA sequences of the imperfect inverted repeat indicated that sequence similarity was high in the 3′-end of the exon and the splice donor site, and in specific regions of the imperfect inverted repeat. In contrast, the region separating the repeats was poorly conserved and of variable length, consistent with earlier deletion experiments demonstrating it to be dispensable for *in vitro* editing (Figure 1A and B) (33–35).

Our phylogenetic sequence analysis was used to predict the consensus secondary structure and identify the fundamental structural features required for the essential, high-efficiency editing reaction at the Q/R site (Figure 1A). Calculated base pairing probabilities were highest around the Q/R and intronic editing sites (>0.8). Closer inspection of the Q/R substrate revealed that most sequence variation that does occur comprises consistent mutations that do not alter basepairing (e.g. AU to GU; including a genomically encoded guanine at the +4 editing site; Figure 1C: green), or a mutation that maintains a mismatch position (GA to AA; Figure 1C: blue) to conserve overall RNA secondary structure. In contrast, a small cluster of mutations in the triplet guanosine (+302 to +304) appears mostly to disrupt base pairing (Figure 1C). Consistent with this finding, introducing an N^2-benzyl modification into the minor groove at the guanosine +303 position does not impact on *in vitro* editing at the Q/R site (36). Together, these data reveal novel aspects of this unique editing substrate and highlight specific regions of double strandedness critical for Q/R editing, thus providing a guide for antisense target design.

Antisense inhibition of an exogenous Q/R editing reporter system

The double stranded nature of A-to-I editing sites implies a substrate requirement for editing that could be targeted by competitive inhibition: hybridization of a steric antisense probe to the ECS to disrupt Adar2 binding and deamination. Potent steric antisense activity of morpholino oligos has been demonstrated on highly structured RNA targets (18–20). Given the extensive duplex structure of the Q/R editing substrate this site was chosen as a poof-of-principle target. A 25-mer morpholino was designed to hybridize to the entire Q/R site ECS (+315 to +324), the binding site of dsRBD1 (+307 to +317) and five unstructured base positions outside the structured RNA to assist in strand invasion of the antisense oligo (Figure 1A: outlined in green; Figure 2; Supplementary Table S2).

To test the antisense approach, we initially used an exogenous reporter system (33–35,37) (Figure 3A: top). This constitutes a fragment of the rat GluA2 gene, encompassing the 3′ half of exon 11 and ~0.5 kb of the proximal portion of the proceeding intron (33). The reporter was transfected into HeLa cells, which have been shown previously to have some A-to-I RNA editing activity (34) and respond well to the Endo-porter morpholino delivery reagent (30). Amplicons of the minigene reporter transcript showed both adenine, and to a lesser extent, guanine at the editing site in the chromatograms obtained by Sanger sequencing (Figure 3B). In addition, digestion with BbvI (GCAGC) restriction enzyme gave two detectable bands corresponding to the predicted fragment sizes (Figure 3C). In contrast, a construct with the edited residue genomically encoded showed only guanine and a ΔECS construct exhibited only an adenine at the editing site (Figure 3A–C). These results validate the test system and confirm the essential role of the ECS in Q/R editing.

Antisense oligo (10 μM) delivered into reporter-expressing HeLa cells resulted in significantly inhibition of Q/R editing compared with vehicle controls (Figure 3D). A dose–response experiment provided a

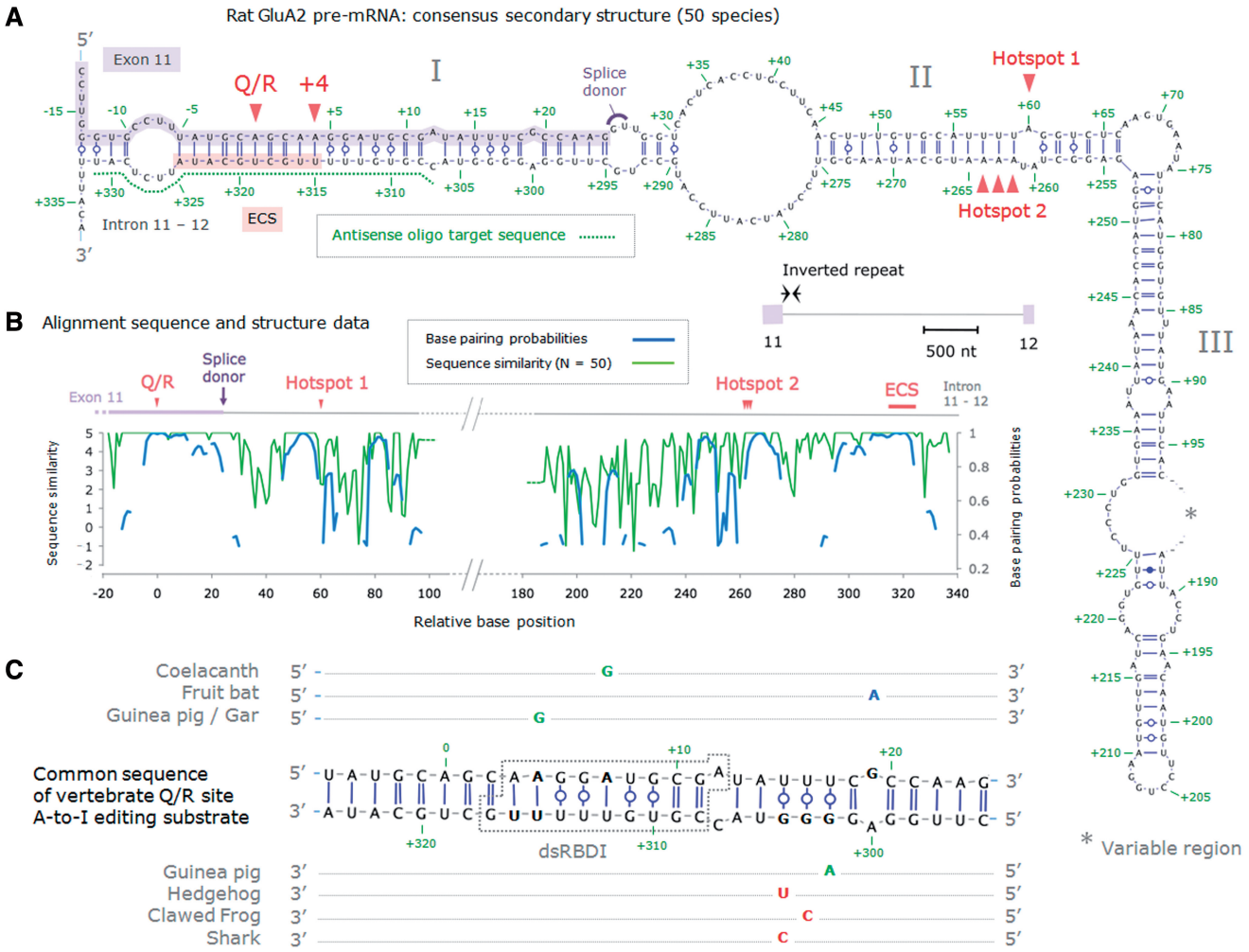

Figure 1. Phylogenetic analysis of the Q/R site substrate. (**A**) The predicted common secondary structure (γ-centroid estimator) of the GluA2 pre-mRNA encompassing the Q/R site for 50 vertebrate species (Supplementary Table S1) mapped onto the rat sequence. Base pairs are rendered according to the Leontis/Westhof nomenclature. The splice donor site and editing sites are annotated in violet and red, respectively. Editing site designations and sequence numbering are as published by the Seeburg laboratory (33): the base position numbering corresponds to that of the aligned mouse sequence with reference to the Q/R site (position = 0). Lilac highlight = exon sequence; salmon highlight = Q/R ECS; dotted green line annotation = antisense morpholino target sequence; grey asterisk = variable region (lacking sequence similarity or a common structure). Roman numerals I–III label prominent, highly conserved helical elements [see (B)]. Inset: Imperfect inverted repeat illustrated on a scaled schematic of the rat *Gria2* gene fragment spanning exons 11–12. (**B**) Line plots summarizing the data relating to (A). Primary axis is for vertebrate sequence similarity (green) and secondary axis is for probabilities of the base pairs shown in the predicted consensus structure (A). Only data for base positions aligned to the rodent sequence are shown (i.e. alignment gaps were deleted). The variable region separating the imperfect inverted repeats showed little to no sequence or structural conservation and therefore was omitted from the plot. A linearized schematic of the rat GluA2 pre-mRNA features is shown above the plot to annotate the base positions. (**C**) Detailed characterization of the minimal Q/R site editing substrate across vertebrates. The mapped Adar2 double-stranded RNA binding domain I (dsRBDI) binding site spans the helical element outlined with a dotted grey line. Vertebrate species that deviate from the common sequences of either strand are shown. The sequence variation is color coded: green font indicates that canonical RNA base pairing is maintained; blue font indicates that a mismatch is maintained and red indicates a change in RNA secondary structure. The more recently available sequences for diploid bony fish species coelacanth and spotted gar were not included in the original alignment used to create (A) and (B). However, their inclusion gives a similar consensus structure when mapped onto the rat sequence.

50% inhibitory concentration (IC_{50}) of ~1.9 μM (Figure 3E and F). In contrast, editing was not affected by any tested concentrations of a standard negative control oligo (Supplementary Table S2; Figure 3E and F) (http://www.gene-tools.com/node/23#standardcontrols).

Together, these experiments indicate that Q/R editing of a minigene reporter can indeed be effectively perturbed using a substrate-targeted antisense oligo. Furthermore, we could demonstrate that this effect was sequence and editing site specific (Supplementary Figure S1A and S2; see also next section). The ability and specificity of the antisense to inhibit Q/R editing of endogenous GluA2 was examined next.

Specific steric antisense inhibition of the endogenous Q/R editing substrate

The neuroblastoma cell line SH-SY5Y expresses GluA2 endogenously, which is edited by Adar2 (38). Morpholinos were delivered over a 16–24 h period before assaying the editing state of the Q/R site. In

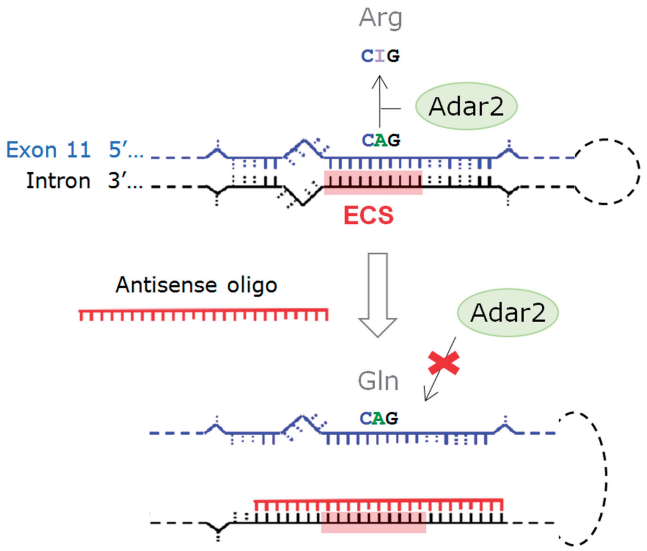

Figure 2. A steric antisense strategy to inhibit an A-to-I editing site. The substrate-targeted strategy is demonstrated for A-to-I editing on a simplified schematic of the GluA2 pre-mRNA Q/R site (see text). Arg = arginine; Gln = glutamine; Adar2 = adenosine deaminase acting on RNA2; CAG is the sequence of the arginine triplet codon targeted by Adar2 for enzymatic deamination to CIG (read as CGG, the glutamine triplet codon).

vehicle controls, GluA2 mRNA was ~85% edited at the Q/R site. Titration of the antisense oligo caused a striking, dose-dependent switch in the editing state of endogenous GluA2 mRNA (Figure 5A: green line). At the highest dose tested (20 μM), the antisense resulted in ~80% drop in the relative quantity of Q/R edited mRNA compared with vehicle delivery control or to the standard negative control oligo (Figure 4A and B). To control for the possibility that differences in solubility could result in varying extents of delivery between antisense and control oligos we used an oligo with equivalent base content to the antisense, but with inverted sequence (Supplementary Table S2). As with the standard negative control oligo, this invert morpholino showed no inhibition (Figure 4A and B). In addition, five mismatches distributed along the length of the antisense sequence (with minimum change to the GC content; Supplementary Table S2) completely abolished the ability of the oligo to inhibit Q/R editing, indicating that sequence specificity was maintained (Figure 4A and B). Furthermore, the antisense was not associated with inhibition of editing in endogenously expressed 5-HT_{2C}R mRNA indicating that a general effect on A-to-I editing is unlikely with up to 10° μM of antisense morpholino (Supplementary Figure S1B). We also obtained the same result for a similar series of control experiments using the exogenous reporter system in HeLa cells (Supplementary Figure S1A and S2).

If the morpholinos are operating *via* a steric mechanism, the above results should be reproducible using a different backbone chemistry, which similarly does not induce RNase-H cleavage or trigger RNA interference. Accordingly, we could reproduce inhibition of the Q/R site using an alternative antisense approach: oligos comprised of 2′-O-Methyl RNA/locked nucleic acid (2′-O-Me/LNA) mixmers (39,40) also interfered with Q/R editing, albeit with reduced efficacy (Supplementary Figure S3).

The dramatic effect of competitive inhibition by morpholinos on the high editing levels of endogenous GluA2 mRNA (~85%) was surprising given that efficacy of a competitive inhibitor would be expected to be lower when basal levels of editing (and thus competing levels of Adar2) are higher. To understand this better we examined editing in the endogenous GluA2 pre-mRNA of SH-SY5Y. Consistent with a recent report (38), the editing state of the Q/R site in SH-SY5Y under control conditions was ~3-fold lower for pre-mRNA than for spliced mRNA (Figure 4C). Analyzing the antisense dose–response data for pre-mRNA indicated that the IC_{50} was very similar to that of the corresponding mRNA (1.8 versus 2.8 μM: pre-mRNA versus mRNA; Figure 5A) suggesting that antisense efficacy was comparable for the two RNA populations. The relationship between editing and splicing was examined next.

Coupling of intronic hotspot 2 and splicing to Q/R site substrate integrity

The data above uncovered a disparity between Q/R editing before and after splicing, which is consistent with earlier reports describing greater splicing efficiency for the Q/R-edited GluA2 pre-mRNA (11,41,42). The antisense approach provided an opportunity to test this relationship further. We plotted dose–response data for ratios of editing in mRNA against those of pre-mRNA; the slope of the resulting plot providing the relative splicing efficiency (Supplementary Figure S6). The data were significantly correlated ($r = 0.86$, $P < 0.0001$, Spearman's rank) and were fit well by a linear function ($R^2 = 0.8$) with a slope corresponding to ~3.8 times more efficient splicing of edited pre-mRNA (Figure 5B). It has been demonstrated recently that the combination of editing at the Q/R site and at intronic hotspot 2 (position +262) is responsible for more efficient splicing of edited GluA2 pre-mRNA (42). Therefore, we analyzed the extent of editing at the intronic hotspots (Figure 5C). Given that these lie in an independent helical element (Figure 1A: helix II) to the Q/R site (Figure 1A: helix I) and antisense target we were surprised to find that hotspot 2 editing (in particular +262) was inhibited by the antisense as efficiently as the Q/R site (Figure 5D). Moreover, the editing at both sites was well-correlated ($r = 0.81$, $P < 0.01$; Spearman's rank; Figure 5E). Therefore, there appears to be a direct coupling of the Q/R site and hotspot 2 that maintains preferential splicing of the Q/R-edited GluA2 pre-mRNA (42).

Editing-coupled splicing efficiency and high basal editing activity safeguard the Q/R site

The low level of editing at the Q/R site of GluA2 pre-mRNA in SH-SY5Y is unlike that in brain, where it often exceeds 95% (Figure 6A; Supplementary Table S3). Similarly, MIN-6, a β-pancreatic cell line, expresses GluA2 with near 100% editing of the Q/R site in GluA2 pre-mRNA (Figure 6A; Supplementary Table S3). In

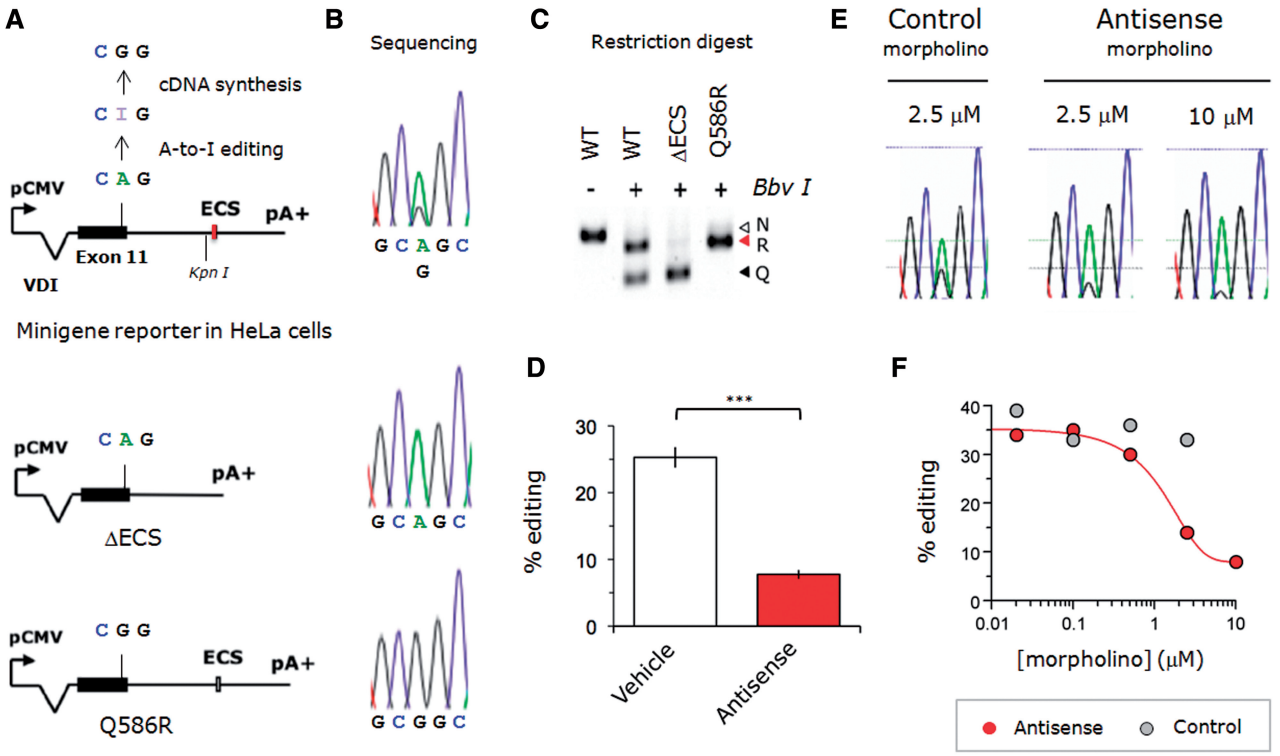

Figure 3. The antisense strategy inhibits editing of a Q/R site minigene reporter. (**A**) Minigene reporter constructs for Q/R editing (top). Note the efficiently spliced vector-derived intron (VDI) located 5′ of the insert used to assist selective amplification of cDNA). The KpnI restriction site was used to create the ΔECS mutant (middle). As a positive control for detection of edited transcripts, we also created a construct with a genomically encoded QR site (bottom). pA+ = polyadenylation signal; pCMV = cytomegalovirus promoter. (**B**) Sequence chromatograms of RT-PCR amplicons for each of the corresponding constructs expressed in HeLa cells. (**C**) The qualitative results obtained in (B) by sequencing are supported by specific enzyme digest. Restriction enzyme (BbvI) digests of RT-PCR amplicons for each construct were loaded on an agarose gel (3%), which was then post-stained with ethidium bromide. The image shown was inverted for clarity. A constitutive BbvI restriction site in the amplicon incorporated by one of the primers served as a control for digestion. N = non-digested fragment; R = edited digestion fragment; Q = unedited digestion fragment. Note that for the WT construct the uncut edited fragment appears more intense than the cut unedited fragment. This is in contrast to what is seen with the same sample by Sanger sequencing. This is likely due to the fact that the level of ethidium bromide staining is a function of the size and the abundance of the DNA fragment. In addition, it is possible that heteroduplexes formed in PCR are not cut effectively by this restriction enzyme. For these reasons we have quantified editing from sequence chromatograms. (**D**) Antisense morpholino provided robust and significant inhibition of Q/R editing of the reporter minigene. Bar graph showing the percentage editing of the reporter minigene with vehicle and with antisense morpholino. The morpholino delivery vehicle was Endo-Porter. The sample size was 3 - 4 transfections. Error bars represent SEM. $***P < 0.001$ (Student's two-tailed unpaired *t*-test with Welch's correction). (**E**) Sequence chromatograms of RT-PCR amplicons derived from HeLa cells expressing the reporter minigene and treated with different doses of standard control morpholino and antisense morpholino. The morpholino delivery vehicle was Endo-Porter (Gene-Tools). (**F**) The peak heights of the sequence chromatograms in (E) are quantified (see 'Materials and Methods' section) and plotted as percentage editing against morpholino concentration on a logarithmic scale. The 10 μM concentration for the control morpholino was not carried out in this experiment. The data points for the antisense treatment were fit with sigmoidal curve using the equation: $d + A/(1 + \exp((x - x_0)/c))$. The IC_{50} was 1.9 μM.

addition, intronic pre-mRNA editing hotspots and the R/G editing site of GluA2 mRNA are processed to levels mirroring neural tissue (Supplementary Table S3). Therefore, we used MIN-6 as a tractable cell system for testing the ability of the antisense to perturb Q/R editing in the background of more neuron-like levels of editing activity. The extent of inhibition by morpholinos was compared with inhibition *via* dominant negative Adar2 mutants. In particular, we over-expressed catalytically inactive (E396A) and dominant negative (EAA) forms of Adar2 fusion protein with enhanced green fluorescent protein (EGFP) (Figure 6B). As MIN-6 cells were irresponsive to the delivery vehicle used for the other cell lines, we delivered morpholinos using electroporation and assayed the editing state of GluA2 pre-mRNA.

MIN-6 cells were electroporated with the Adar2 mutants, allowed to express for 3 days, then EGFP-positive cells were collected by fluorescence-activated cell sorting (Figure 6C). The E396A mutant of *Drosophila* Adar has been shown previously to inhibit editing up to 60% for some targets *in vivo* (43). For the Q/R site, we observe only a modest 5% drop in Q/R pre-mRNA editing compared to EGFP alone (Figure 6C). In the dominant negative construct, mutations of key lysine residues (**KK**XXX**K**) in both dsRBDs to **EA**XXX**A** has been proposed to act in a dominant negative fashion by sequestering endogenous Adar2 into non-functional heterodimers (44); we detected a ~3.5-fold greater inhibition by this mutant compared with E396A. However, overall levels of pre-mRNA editing were still as high as 83%, reflecting the unique editing efficiency of the AMPAR Q/R site. Similarly, the antisense oligo reduced pre-mRNA editing to 86%. To confirm that the results were not due to one of the *Gria2* alleles having a

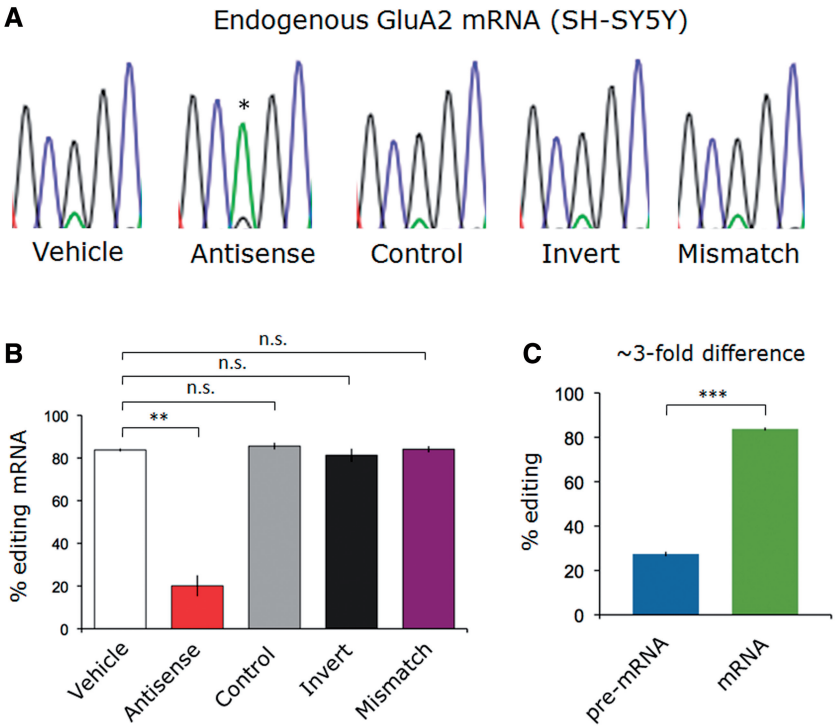

Figure 4. Potent inhibition of the endogenous Q/R site editing in SH-SY5Y cells. (**A**) Effective and sequence-specific inhibition of Q/R editing in mRNA of SH-SY5Y. Sequence chromatograms for SH-SY5Y cells transfected with morpholinos delivered at 20 μM using Endo-Porter vehicle. Sequence specificity was maintained in mismatch control at this relatively high concentration. Asterisk indicates the adenine peak in the antisense morpholino sample trace. (**B**) The inhibition of Q/R editing in SH-SY5Y mRNA was highly significant. Morpholino concentrations were 20 μM. Error bars represent SEM. The sample size for each treatment was 3. $^{**}P < 0.01$, n.s. = not significant ($P < 0.0001$, one-way ANOVA with Dunnett's post-test comparison: morpholino versus vehicle control). (**C**) Graph illustrating the percentage Q/R editing of GluA2 pre-mRNA and mRNA in control dishes of SH-SY5Y. The 3-fold difference is highly significant (two-tailed *t*-test). $^{***}P < 0.001$.

genomically encoded guanine at the Q/R editing position (as occurs in the *Gria2β* paralogue in Teleost fish) we examined the editing state of the genomic DNA. Restriction digest with TauI (GCGGC) revealed complete editing of pre-mRNA but only one band (corresponding to the unedited sequence: GCAGC) in genomic DNA (Figure 6E), which ruled out this possibility. To account for GluA2 mRNA turnover in MIN-6 cells we tested a range of harvesting time points post-electroporation for the antisense oligo and found that the largest drop (~45%) in Q/R editing of GluA2 pre-mRNA at the earliest time point (at 12 h), and a gradual increase in editing over time, which likely reflects dilution of the antisense oligo during cell divisions (Figure 6D). The changes in Q/R editing of pre-mRNA was accompanied by only small changes in editing of the spliced mRNA (Figure 6D).

DISCUSSION

Here, we describe a strategy to selectively target specific A-to-I editing sites for inhibition. Steric antisense morpholinos designed to hybridize to the ECS of the GluA2 Q/R site substrate specifically and effectively perturbed editing at this site in the background of lower A-to-I editing activity, which is commonly seen with most other A-to-I editing targets. In addition, the antisense approach revealed a tight coupling of intronic hotspot 2 to the Q/R site, which likely ensures more efficient splicing of Q/R edited pre-mRNA. This 'safe-guard', potentially unique to the Q/R site (Supplementary Figure S4), contributes to the difficulty in perturbing Q/R editing in the background of high-editing activity. This novel antisense approach could be used to identify currently unexplored functions of select A-to-I editing sites.

We used morpholino backbone chemistry to make steric block antisense oligos. Unmodified DNA and RNA oligos are rapidly degraded in biological systems by enzymatic cleavage of the phosphodiester bond (Supplementary Figure S3B, R = O^-) and are prone to hydrolysis due to the presence of a hydroxyl group on the 2′-carbon of the ribose sugar (Supplementary Figure S3B, X = OH). Some leading backbone modifications for steric antisense applications include peptide nucleic acids, morpholinos and 2′-O-methyl RNA/LNA mixmers. For example, morpholinos are widely used to modify pre-mRNA splicing, block mRNA translation and inhibit miRNA maturation or activity (16,17) and have been used in several model organisms, such as sea urchins, zebrafish, frogs, chicks and mice (45). We add another application to this list: steric antisense inhibition of RNA editing. The application of new antisense delivery systems [e.g. Tat peptides (39,40)] with the current strategy will facilitate evaluation of editing sites *in vivo*.

In our application of the antisense tool, our data emphasizes the robust nature of this functionally critical A-to-I

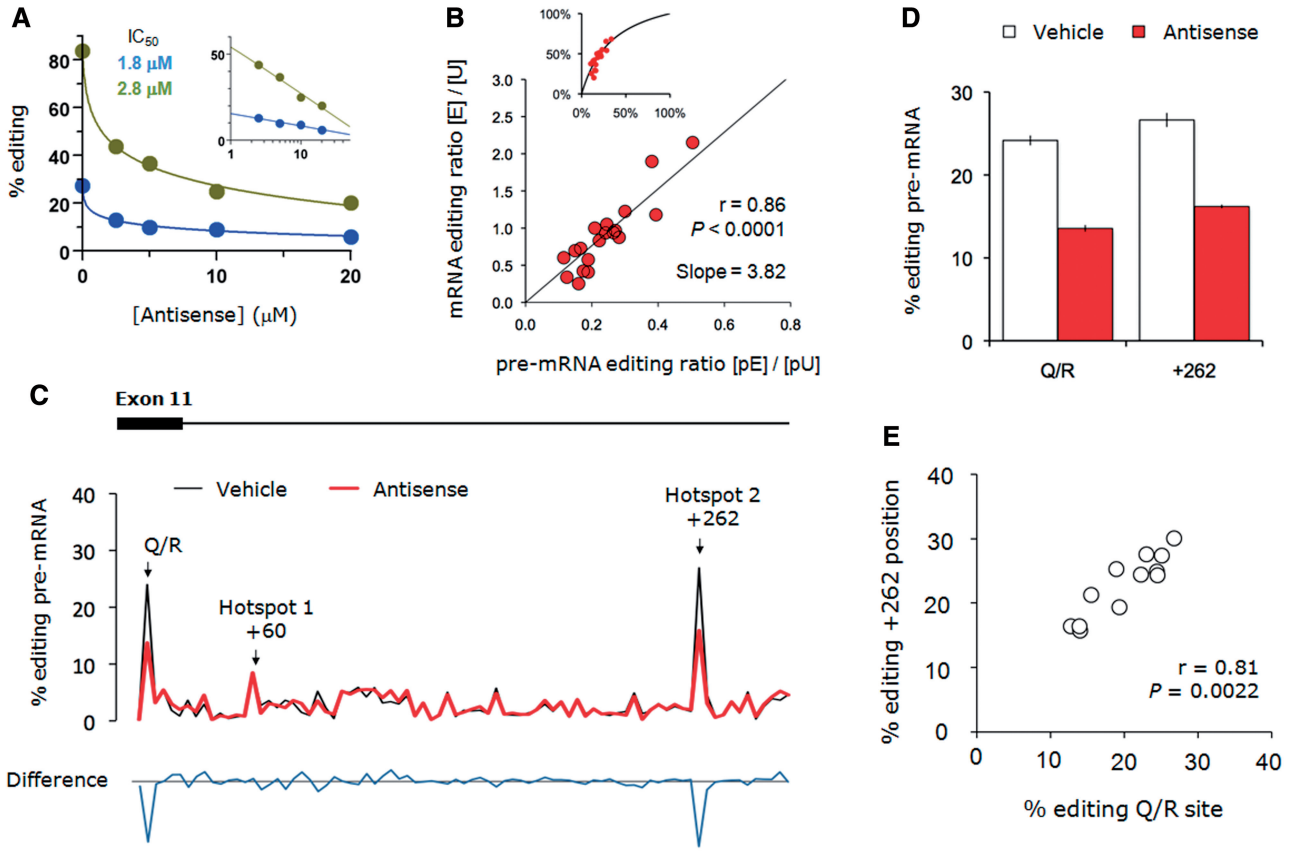

Figure 5. Coupling of inhibition at the Q/R site and editing at intronic hotspot 2. (**A**) Dose-dependent inhibition of Q/R editing of SH-SY5Y GluA2 pre-mRNA (blue) and mRNA (green). Error bars represent SEM. The data points were fit with the equation $a+b*\ln(x+c)$. The IC_{50} values for pre-mRNA and mRNA were 1.8 and 2.8 μM, respectively. The inset shows the data normalized to vehicle control and plot against concentration on a logarithmic scale. (**B**) Preferential splicing of the Q/R-edited pre-mRNA probed using the antisense. The editing ratios from dose–response experiments were corrected for non-linearities of mixed sequence peaks using standard curves created with plasmid mixtures and the corrected data were plot on a scatter graph. The data points were fit by least squares linear regression through the origin ($R^2 = 0.80$) and correlation tested with Spearman's rank. The slope corresponds to the fold difference in splicing efficiency for edited pre-mRNA compared with unedited pre-mRNA (Supplementary Figure S6). The inset shows how the data and the fit look when editing is expressed as percentages; the fit becomes hyperbolic. Note that the slope of the relationship decreases as the % pre-mRNA editing increases. (**C**) Quantification at 'editing' ratios at all adenine positions in the imperfect inverted repeat upto position +305. Black line is vehicle control, red line is antisense. The exon–intron structure is illustrated above the plot. The difference in peak heights is plot below (blue line). (**D**) A bar graph showing editing at the Q/R site and intronic editing hotspot 2 (position +262) in GluA2 pre-mRNA with antisense morpholino or Endo-porter vehicle only. (**E**) Scatter plot of editing at the intronic editing hotspot 2 (position +262) in GluA2 pre-mRNA versus editing at the Q/R site with varying dose of antisense morpholino. The data points were tested for correlation using Spearman's rank.

editing substrate. Intact preferential splicing of edited pre-mRNA combined with high-editing activity will make transient fluctuations of Adar2 unlikely to lead to significant changes in editing status of spliced (protein coding) transcript (42). This is supported by our experiments using siRNAs to knockdown Adar2 in cultured neurons (Supplementary Figure S5). Recently, it was shown that increased splicing efficiency requires edited positions at both the Q/R site and hotspot 2 (43). Our antisense approach provides evidence for a coupling between hotspot 2 and Q/R substrate integrity. Consistent with the essential requirement for editing the Q/R site, we show that the hotspot 2 sequence and structure of the associated helical element (Figure 1A: helix II) is almost as well-conserved as the Q/R site substrate itself (Figure 1A: helix I; Figure 1B). This observation for coupling between the editing sites is also supported by earlier ECS mutagenesis experiments (33). The absence of obvious coupling to the +60 site on the complementary strand of hotspot 2 is not surprising given that it is almost exclusively an Adar1 target (11).

Positive and negative coupling between relatively distant editing sites and RNA secondary structures has been shown recently for the Adar2, 5-HT_{2C}R, GluK2 and Gabra3 substrates (47,48). One possible explanation for the positive coupling observed in GluA2 could be as follows: Adar2 binds the Q/R substrate and dimerizes (44,45), the second subunit then binds and edits hotspot 2. Such avidity would be consistent with the high levels of pre-mRNA editing typically observed for the Q/R site compared to some other A-to-I editing sites. Consistent with this *in vitro* editing of a minimal Q/R substrate (like the one shown in Figure 1C) is less efficient than that of the complete pre-mRNA *in vivo* (36). However, in the absence of structural information, proof for such a mechanism remains unexplored.

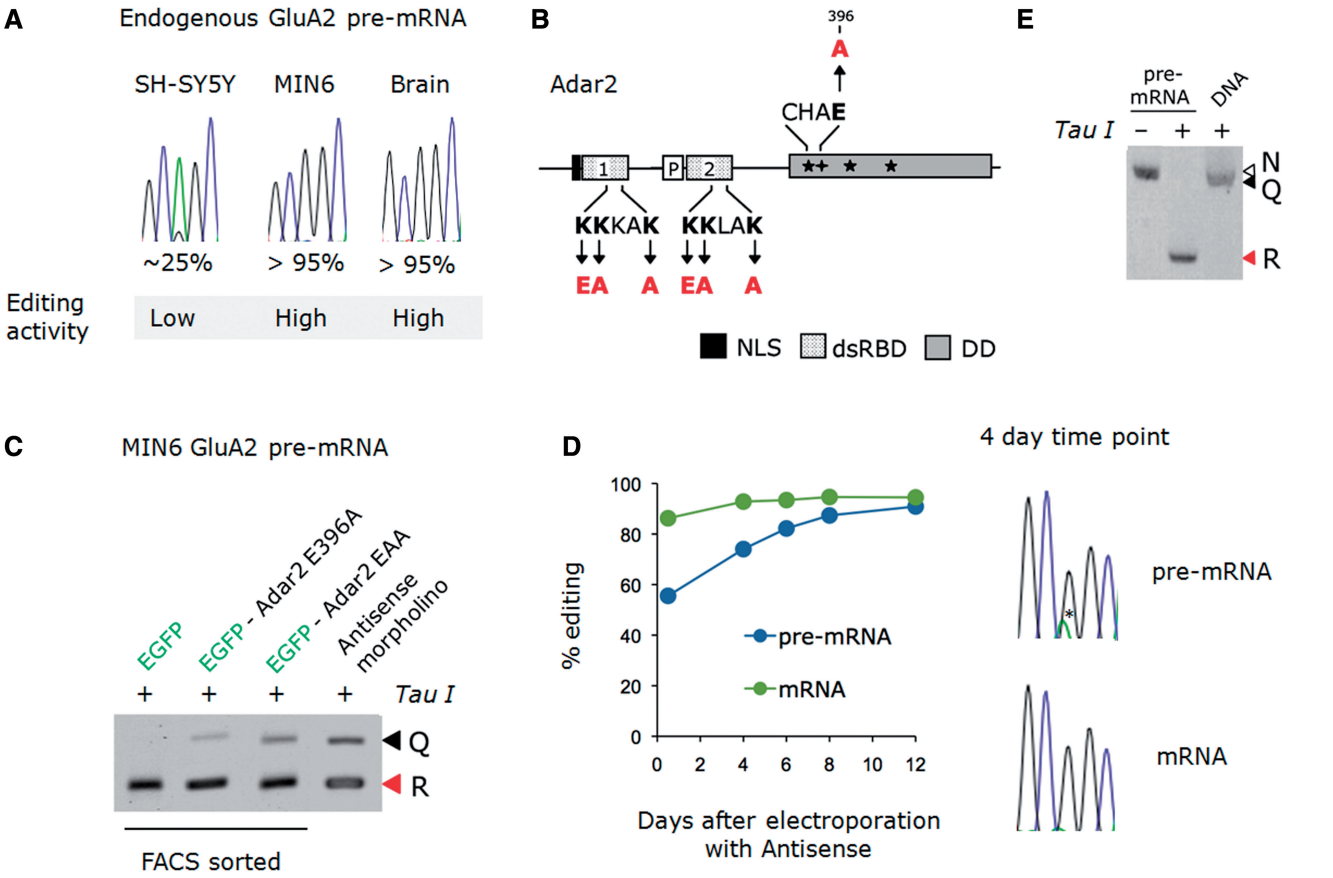

Figure 6. Preferential splicing of Q/R-edited pre-mRNA prevents antisense inhibition in MIN-6 cells. (**A**) Example sequence chromatogram traces of the Q/R site from pre-mRNA sequence amplified from cDNA. As the Q/R site is exclusively edited by Adar2, this indicates that SH-SY5Y and MIN-6 have low-and high-editing activity, respectively. As with MIN-6, Adar2 editing activity in the brain is high. (**B**) A schematic illustration of the Adar2 protein and the position of the mutations introduced by cloning to create inactive (E396A) and dominant-negative (EAA) EGFP-ADAR2 mutants. The amino terminal EGFP tag is not illustrated. The Adar2b protein is 711 amino acids in length. Adar2 = adenosine deaminase acting on RNA 2; NLS = nuclear localization signal; DD = deaminase domain. (**C**) Inhibition of Q/R editing in MIN-6 GluA2 is observed with Adar2 mutants (positive controls) and antisense morpholino. The negative control was empty vector. Restriction enzyme (TauI) digests were performed on RT-PCR fragments amplified from pre-mRNA and loaded on an agarose gel (2%), which was then post-stained with ethidium bromide. The high molecular weight corresponds to GluA2 unedited at the Q/R site. R = edited digestion fragment; Q = unedited digestion fragment. Cells were transfected by electroporation. (**D**) Inhibition of endogenous editing can be detected as early as 12 h after antisense morpholino transfection. Time course determination of changes in MIN-6 GluA2 pre-mRNA and mRNA editing at the Q/R site are shown for a single experiment. Data points represent the percentage editing determined from the peak heights of sequence chromatograms. Examples of sequence traces from the 4-day time point are shown on the right. Cells were transfected by electroporation. (**E**) Digestion of PCR product from MIN-6 cDNA and genomic DNA with an enzyme (TauI) that recognizes the edited sequence (GCGGC) confirms that both genomic alleles encode a glutamine (Q) at the Q/R site. A constitutive TauI restriction site in the amplicon incorporated by one of the primers served as a control for digestion. N = non-digested fragment; R = edited digestion fragment; Q = unedited digestion fragment.

Morpholino oligos are typically used to disrupt splicing by sterically blocking splice sites. For example, by hybridizing to the donor splice site morpholinos prevent base pairing of the U1 snRNA and thus assembly of the spliceosome. The antisense target in our study is around ~290 nucleotides downstream of the donor splice site. In addition, although the target and splice donor are on the same helical element of the secondary structure, the nearest end of the target is around 12 bp from the start of the splice site. Furthermore, splicing occurs more rapidly for Q/R edited pre-mRNA because editing and splicing are co-ordinated by the C-terminal domain of RNA polymerase II (41,49). As a consequence, binding of a high-affinity antisense probe is less likely for the edited pre-mRNA. Therefore, a direct effect of the antisense on donor splice site recognition could be biased for the unedited pre-mRNA and predict differences in the IC_{50} for editing in pre-mRNA versus mRNA resulting in dose-dependent deviations from the model described in Supplementary Figure S6, which we do not observe (Figure 5A and B). Together, it seems unlikely that the antisense has a direct impact on splicing but rather exerts a specific effect on editing.

In summary, this antisense approach should open up in-depth characterization of other A-to-I editing sites.

SUPPLEMENTARY DATA

Supplementary Data are available at NAR Online: Supplementary Tables 1–3 and Supplementary Figures 1–6.

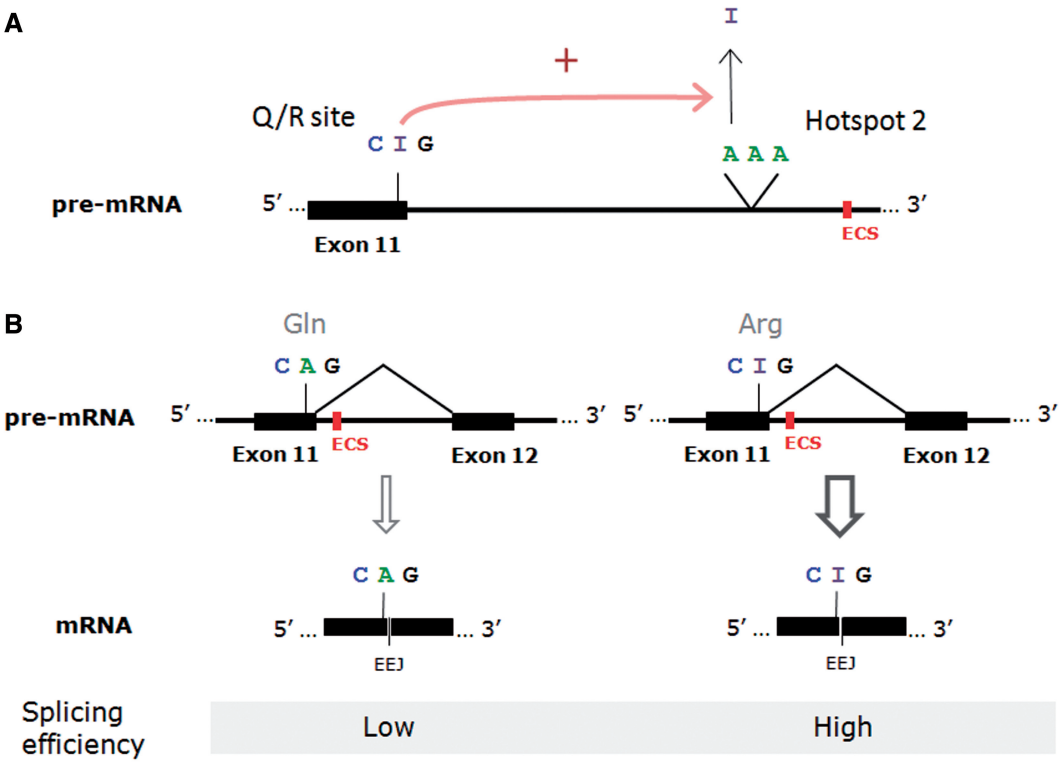

Figure 7. Summary of GluA2 Q/R substrate properties: (**A**) Illustrating the positive coupling between the editing at the Q/R site and hotspot 2 revealed by the antisense; (**B**) Illustrating that the larger fraction of editing apparent in mRNA results from more efficient splicing of edited pre-mRNA. Coupling of the intronic editing hotspot 2 to the Q/R editing site is probably responsible for the change in pre-mRNA splicing efficiency.

ACKNOWLEDGEMENTS

We thank Mike Gait for advice during early stages of this project and Martin Fabani for his help with experimentation using the alternative antisense chemistry. We are also grateful to Jon Moulton who advised in morpholino design. We are grateful to Shanta Persaud for providing MIN-6 cells and Yvonne Vallis for SH-SY5Y cells.

FUNDING

Medical Research Council [U105174197 to A.C.P., A.B. and I.H.G.]; Royal Society (to I.H.G.). Funding for open access charge: Medical Research Council.

Conflict of interest statement. None declared.

REFERENCES

1. Jepson,J.E. and Reenan,R.A. (2008) RNA editing in regulating gene expression in the brain. *Biochim. Biophys. Acta*, **1779**, 459–470.
2. Tariq,A. and Jantsch,M.F. (2012) Transcript diversification in the nervous system: A to I RNA editing in CNS function and disease development. *Front. Neurosci.*, **6**, 99.
3. Rosenthal,J.J. and Seeburg,P.H. (2012) A-to-I RNA editing: effects on proteins key to neural excitability. *Neuron*, **74**, 432–439.
4. Bass,B.L. (2002) RNA editing by adenosine deaminases that act on RNA. *Annu. Rev. Biochem.*, **71**, 817–846.
5. Hogg,M., Paro,S., Keegan,L.P. and O'Connell,M.A. (2011) RNA editing by mammalian ADARs. *Adv. Genet.*, **73**, 87–120.
6. Sommer,B., Kohler,M., Sprengel,R. and Seeburg,P.H. (1991) RNA editing in brain controls a determinant of ion flow in glutamate-gated channels. *Cell*, **67**, 11–19.
7. Traynelis,S.F., Wollmuth,L.P., McBain,C.J., Menniti,F.S., Vance,K.M., Ogden,K.K., Hansen,K.B., Yuan,H., Myers,S.J., Dingledine,R. *et al.* (2010) Glutamate receptor ion channels: structure, regulation, and function. *Pharmacol. Rev.*, **62**, 405–496.
8. Greger,I.H., Khatri,L., Kong,X. and Ziff,E.B. (2003) AMPA receptor tetramerization is mediated by Q/R editing. *Neuron*, **40**, 763–774.
9. Feldmeyer,D., Kask,K., Brusa,R., Kornau,H.C., Kolhekar,R., Rozov,A., Burnashev,N., Jensen,V., Hvalby,O., Sprengel,R. *et al.* (1999) Neurological dysfunctions in mice expressing different levels of the Q/R site-unedited AMPAR subunit GluR-B. *Nat. Neurosci.*, **2**, 57–64.
10. Brusa,R., Zimmermann,F., Koh,D.S., Feldmeyer,D., Gass,P., Seeburg,P.H. and Sprengel,R. (1995) Early-onset epilepsy and postnatal lethality associated with an editing-deficient GluR-B allele in mice. *Science*, **270**, 1677–1680.
11. Higuchi,M., Maas,S., Single,F.N., Hartner,J., Rozov,A., Burnashev,N., Feldmeyer,D., Sprengel,R. and Seeburg,P.H. (2000) Point mutation in an AMPA receptor gene rescues lethality in mice deficient in the RNA-editing enzyme *Adar2*. *Nature*, **406**, 78–81.
12. Maas,S., Kawahara,Y., Tamburro,K.M. and Nishikura,K. (2006) A-to-I RNA editing and human disease. *RNA Biol.*, **3**, 1–9.
13. Kwak,S. and Weiss,J.H. (2006) Calcium-permeable AMPA channels in neurodegenerative disease and ischemia. *Curr. Opin. Neurobiol.*, **16**, 281–287.
14. Reenan,R.A. (2001) The RNA world meets behavior: A–>I pre-mRNA editing in animals. *Trends Genet.*, **17**, 53–56.
15. Peng,Z., Cheng,Y., Tan,B.C., Kang,L., Tian,Z., Zhu,Y., Zhang,W., Liang,Y., Hu,X., Tan,X. *et al.* (2012) Comprehensive analysis of RNA-Seq data reveals extensive RNA editing in a human transcriptome. *Nat. Biotechnol.*, **30**, 253–260.

16. Eisen,J.S. and Smith,J.C. (2008) Controlling morpholino experiments: don't stop making antisense. *Development*, **135**, 1735–1743.
17. Moulton,J.D. and Yan,Y.L. (2008) Using Morpholinos to control gene expression. *Curr. Protoc. Mol. Biol.*, Chapter 26: Unit 26.8.
18. Jubin,R., Vantuno,N.E., Kieft,J.S., Murray,M.G., Doudna,J.A., Lau,J.Y. and Baroudy,B.M. (2000) Hepatitis C virus internal ribosome entry site (IRES) stem loop IIId contains a phylogenetically conserved GGG triplet essential for translation and IRES folding. *J. Virol.*, **74**, 10430–10437.
19. Summerton,J. (1999) Morpholino antisense oligomers: the case for an RNase H-independent structural type. *Biochim. Biophys. Acta*, **1489**, 141–158.
20. Summerton,J., Stein,D., Huang,S.B., Matthews,P., Weller,D. and Partridge,M. (1997) Morpholino and phosphorothioate antisense oligomers compared in cell-free and in-cell systems. *Antisense Nucleic Acid Drug Dev.*, **7**, 63–70.
21. Rice,P., Longden,I. and Bleasby,A. (2000) EMBOSS: the European Molecular Biology Open Software Suite. *Trends Genet.*, **16**, 276–277.
22. Carver,T. and Bleasby,A. (2003) The design of Jemboss: a graphical user interface to EMBOSS. *Bioinformatics*, **19**, 1837–1843.
23. Altschul,S.F., Madden,T.L., Schaffer,A.A., Zhang,J., Zhang,Z., Miller,W. and Lipman,D.J. (1997) Gapped BLAST and PSI-BLAST: a new generation of protein database search programs. *Nucleic Acids Res.*, **25**, 3389–3402.
24. Birney,E., Andrews,T.D., Bevan,P., Caccamo,M., Chen,Y., Clarke,L., Coates,G., Cuff,J., Curwen,V., Cutts,T. *et al.* (2004) An overview of Ensembl. *Genome Res.*, **14**, 925–928.
25. Kent,W.J. (2002) BLAT—the BLAST-like alignment tool. *Genome Res.*, **12**, 656–664.
26. Venkatesh,B., Kirkness,E.F., Loh,Y.H., Halpern,A.L., Lee,A.P., Johnson,J., Dandona,N., Viswanathan,L.D., Tay,A., Venter,J.C. *et al.* (2007) Survey sequencing and comparative analysis of the elephant shark (*Callorhinchus milii*) genome. *PLoS Biol.*, **5**, e101.
27. Katoh,K., Kuma,K., Miyata,T. and Toh,H. (2005) Improvement in the accuracy of multiple sequence alignment program MAFFT. *Genome Inform.*, **16**, 22–33.
28. Hamada,M., Sato,K. and Asai,K. (2011) Improving the accuracy of predicting secondary structure for aligned RNA sequences. *Nucleic Acids Res.*, **39**, 393–402.
29. Darty,K., Denise,A. and Ponty,Y. (2009) VARNA: interactive drawing and editing of the RNA secondary structure. *Bioinformatics*, **25**, 1974–1975.
30. Summerton,J.E. (2005) Endo-Porter: a novel reagent for safe, effective delivery of substances into cells. *Ann. N. Y. Acad. Sci.*, **1058**, 62–75.
31. Dominski,Z. and Kole,R. (1993) Restoration of correct splicing in thalassemic pre-mRNA by antisense oligonucleotides. *Proc. Natl Acad. Sci. USA*, **90**, 8673–8677.
32. Ge,B., Gurd,S., Gaudin,T., Dore,C., Lepage,P., Harmsen,E., Hudson,T.J. and Pastinen,T. (2005) Survey of allelic expression using EST mining. *Genome Res.*, **15**, 1584–1591.
33. Higuchi,M., Single,F.N., Kohler,M., Sommer,B., Sprengel,R. and Seeburg,P.H. (1993) RNA editing of AMPA receptor subunit GluR-B: a base-paired intron-exon structure determines position and efficiency. *Cell*, **75**, 1361–1370.
34. Rueter,S.M., Burns,C.M., Coode,S.A., Mookherjee,P. and Emeson,R.B. (1995) Glutamate receptor RNA editing in vitro by enzymatic conversion of adenosine to inosine. *Science*, **267**, 1491–1494.
35. Yang,J.H., Sklar,P., Axel,R. and Maniatis,T. (1995) Editing of glutamate receptor subunit B pre-mRNA in vitro by site-specific deamination of adenosine. *Nature*, **374**, 77–81.
36. Stephens,O.M., Haudenschild,B.L. and Beal,P.A. (2004) The binding selectivity of *Adar2*'s dsRBMs contributes to RNA-editing selectivity. *Chem. Biol.*, **11**, 1239–1250.
37. Egebjerg,J., Kukekov,V. and Heinemann,S.F. (1994) Intron sequence directs RNA editing of the glutamate receptor subunit GluR2 coding sequence. *Proc. Natl Acad. Sci. USA*, **91**, 10270–10274.
38. Yamashita,T., Tadami,C., Nishimoto,Y., Hideyama,T., Kimura,D., Suzuki,T. and Kwak,S. (2012) RNA editing of the Q/R site of GluA2 in different cultured cell lines that constitutively express different levels of RNA editing enzyme *Adar2*. *Neurosci. Res.*, **73**, 42–48.
39. Arzumanov,A., Stetsenko,D.A., Malakhov,A.D., Reichelt,S., Sorensen,M.D., Babu,B.R., Wengel,J. and Gait,M.J. (2003) A structure-activity study of the inhibition of HIV-1 Tat-dependent trans-activation by mixmer 2′-O-methyl oligoribonucleotides containing locked nucleic acid (LNA), alpha-L-LNA, or 2′-thio-LNA residues. *Oligonucleotides*, **13**, 435–453.
40. Arzumanov,A., Walsh,A.P., Rajwanshi,V.K., Kumar,R., Wengel,J. and Gait,M.J. (2001) Inhibition of HIV-1 Tat-dependent trans activation by steric block chimeric 2′-O-methyl/LNA oligoribonucleotides. *Biochemistry*, **40**, 14645–14654.
41. Ryman,K., Fong,N., Bratt,E., Bentley,D.L. and Ohman,M. (2007) The C-terminal domain of RNA Pol II helps ensure that editing precedes splicing of the GluR-B transcript. *RNA*, **13**, 1071–1078.
42. Balik,A., Penn,A.C., Nemoda,Z. and Greger,I.H. (2012) Activity-regulated RNA editing in select neuronal subfields in hippocampus. *Nucleic Acids Res.*, **41**, 1124–1134.
43. Schoft,V.K., Schopoff,S. and Jantsch,M.F. (2007) Regulation of glutamate receptor B pre-mRNA splicing by RNA editing. *Nucleic Acids Res.*, **35**, 3723–3732.
44. Gallo,A., Keegan,L.P., Ring,G.M. and O'Connell,M.A. (2003) An ADAR that edits transcripts encoding ion channel subunits functions as a dimer. *EMBO J.*, **22**, 3421–3430.
45. Valente,L. and Nishikura,K. (2007) RNA binding-independent dimerization of adenosine deaminases acting on RNA and dominant negative effects of nonfunctional subunits on dimer functions. *J. Biol. Chem.*, **282**, 16054–16061.
46. Heasman,J. (2002) Morpholino oligos: making sense of antisense? *Dev. Biol.*, **243**, 209–214.
47. Daniel,C., Veno,M.T., Ekdahl,Y., Kjems,J. and Ohman,M. (2012) A distant cis acting intronic element induces site-selective RNA editing. *Nucleic Acids Res.*, **40**, 9876–9886.
48. Enstero,M., Daniel,C., Wahlstedt,H., Major,F. and Ohman,M. (2009) Recognition and coupling of A-to-I edited sites are determined by the tertiary structure of the RNA. *Nucleic Acids Res.*, **37**, 6916–6926.
49. Laurencikiene,J., Kallman,A.M., Fong,N., Bentley,D.L. and Ohman,M. (2006) RNA editing and alternative splicing: the importance of co-transcriptional coordination. *EMBO Rep.*, **7**, 303–307.

Supplemental Material

Inventory of Supplemental Material

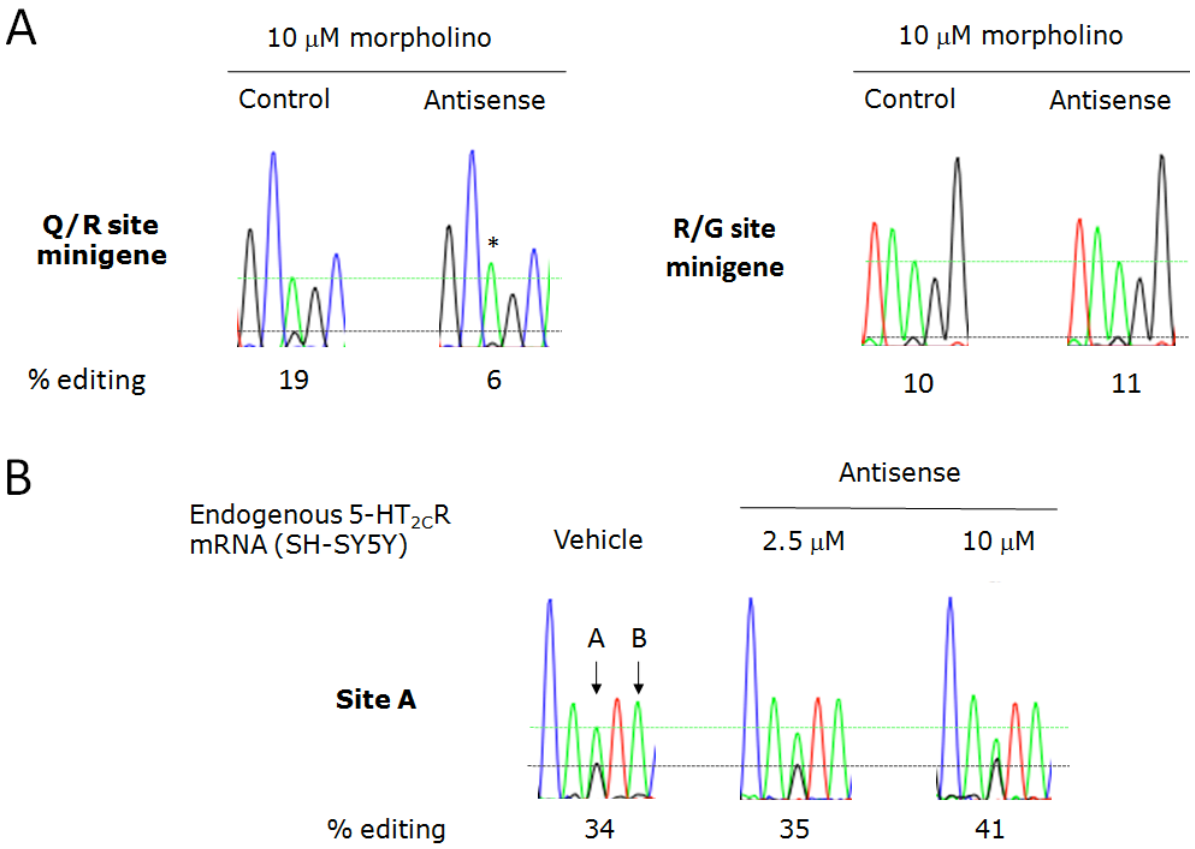

Figure S1

Antisense morpholino directed against the Q/R editing substrate is editing site specific.

A. Experiment showing the effect of 10 μM standard negative control and Q/R-substrate antisense morpholino on the extent of editing in Q/R and R/G site minigene transcripts expressed in HeLa cells. Quantification of editing from peak heights is shown below the DNA sequence chromatograms. Editing inhibition is only seen in the antisense condition for the Q/R site. We reproduced these findings in a separate experiment (R/G site editing: control = 9 %, n = 2; antisense = 9 %, n = 2).

B. Experiment showing the effect of Q/R-substrate antisense morpholino on the extent of editing at site A of serotonin receptor 5-HT_{2C} R mRNA endogenously expressed in SH-SY5Y cells. Quantification of editing from peak heights is shown below the DNA sequence chromatograms. No inhibition of editing was apparent in the antisense conditions (Site A editing: vehicle = 33 %, n = 2; 10 μM antisense = 37 %, n = 2), suggesting that editing site specificity was maintained for the experiments presented in Figs 3 and 4, at least upto a morpholino concentration of 10 μM. Neither the Adar1 specific site B nor the other editing sites of this gene (not shown) were reliably and/or robustly edited in this cell line. Vehicle condition was the morpholino delivery reagent (Endoporter) only.

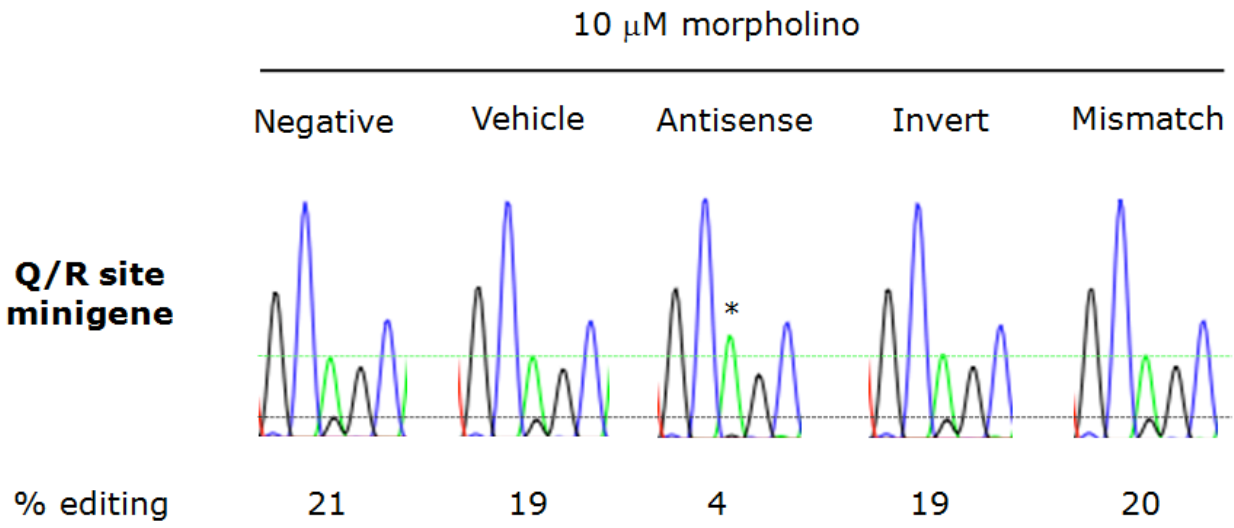

Figure S2

Controls for antisense morpholino directed against Q/R editing of minigene transcript expressed in HeLa cells.

Experiment showing the extent of editing at the Q/R site in minigene transcripts expressed in HeLa cells under different conditions: Negative = No vehicle or morpholino; Vehicle = morpholino delivery reagent (Endoporter) only; Antisense = Q/R-substrate targeted morpholino; Invert = morpholino like antisense but with inverted sequence; Mismatch = morpholino like antisense but with 5 mismatches. Editing inhibition is only seen in the antisense condition indicating that effect in the minigene reporter system was sequence-specific. Quantification of editing from peak heights is shown below the DNA sequence chromatograms.

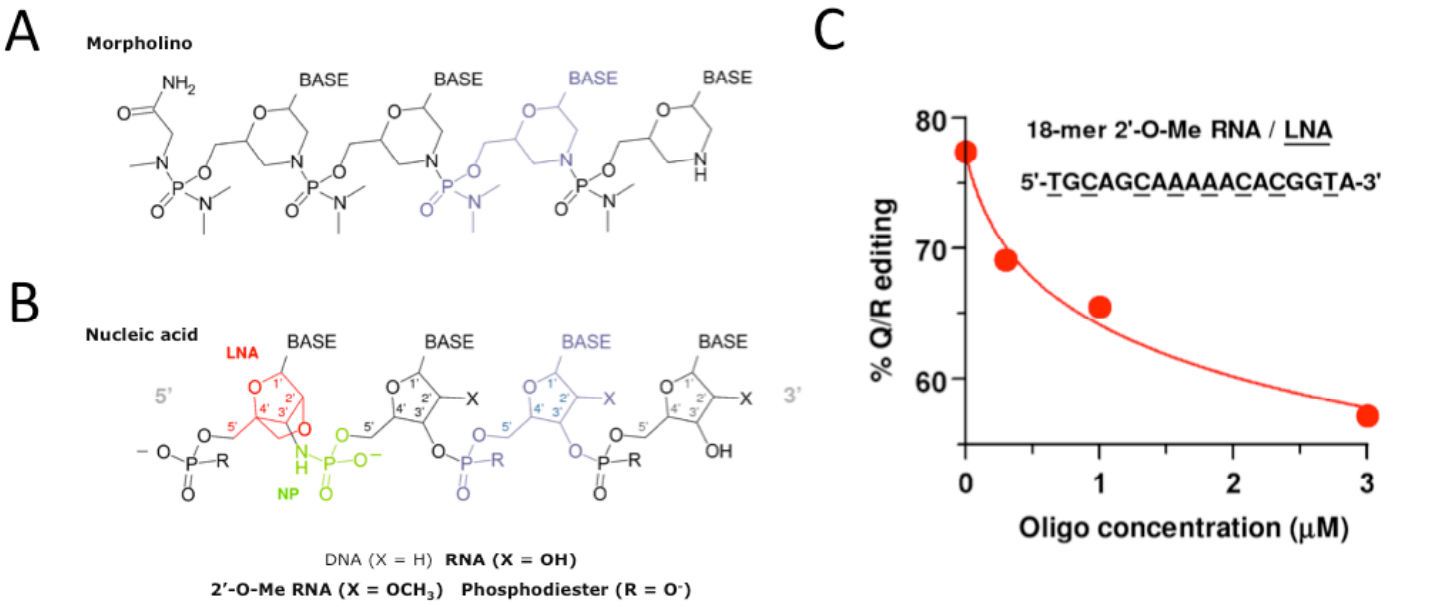

Figure S3

Alternative steric antisense chemistry inhibits editing of the Q/R site in GluA2 mRNA endogenous to SH-SY5Y.

A. The chemical structure of a morpholino backbone. The shown structure is 4 bases in length and is depicted in what is equivalent to the 5'→3' direction in nucleic acids.

B. The chemical structure of a nucleic acid backbone. The shown structure is 4 bases in length in the 5'→3' direction. To illustrate some common steric antisense modifications of the oligos, the 5' sugar is exchanged for locked nucleic acid (LNA), and the 5' internucleoside linkage is exchanged for N3'-P5' phosphoramidate (NP). The alternative antisense oligo chemistry used in Figure S3 was a mixmer of 2'-O-Methyl and LNA sugar modifications with standard phosphodiester linkages. Chemical structures were created with Symyx Draw 3.1. The numbers of the ribose backbone are assigned according to IUPAC conventions.

C. Dose-dependent inhibition of Q/R editing in SH-SY5Y GluR2 mRNA with a 2'-O-Me / LNA steric antisense oligo (see Figure S3B). The data points were fit with the equation a+b*ln(x+c) where a = 64.9, b = -6.27 and c = 0.141. Cells were transfected by electroporation. The sequence of the oligo is shown as an inset in the graph. Backbone sugars replaced with LNA are underlined in the sequence; the remaining ribose sugars had the 2'-O-Me modification. All linkages were phosphodiester.

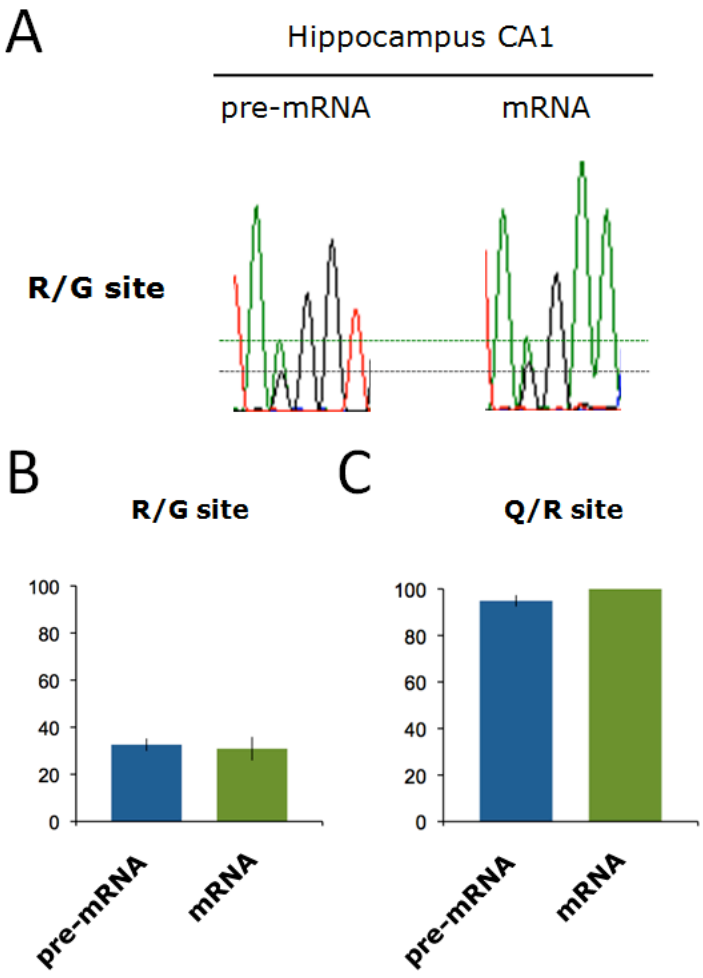

Figure S4

Selective splicing of edited GluA2 pre-mRNA is not observed for the R/G site in region CA1 microdissected from organotypic hippocampal slice.

A. Note the concurrence of GluA2 R/G site editing state in pre-mRNA and spliced mRNA from the example DNA sequence chromatograms. Total RNA was harvested from microdissected CA1 subfield of a cultured hippocampal slice.

B. Summary of replicate data for experiment shown in Fig S4A (n = 3).

C. Summary of replicate data for a similar experiment but for the Q/R site (n = 3). Note that editing of the Q/R site in pre-mRNA is very high (95 % vs 100 % in mRNA), and thus the selective splicing of Q/R-edited transcripts is not readily apparent here. Compare with Fig 3A, where the bias is revealed in SH-SY5Y cells, which have lower endogenous A-to-I editing activity.

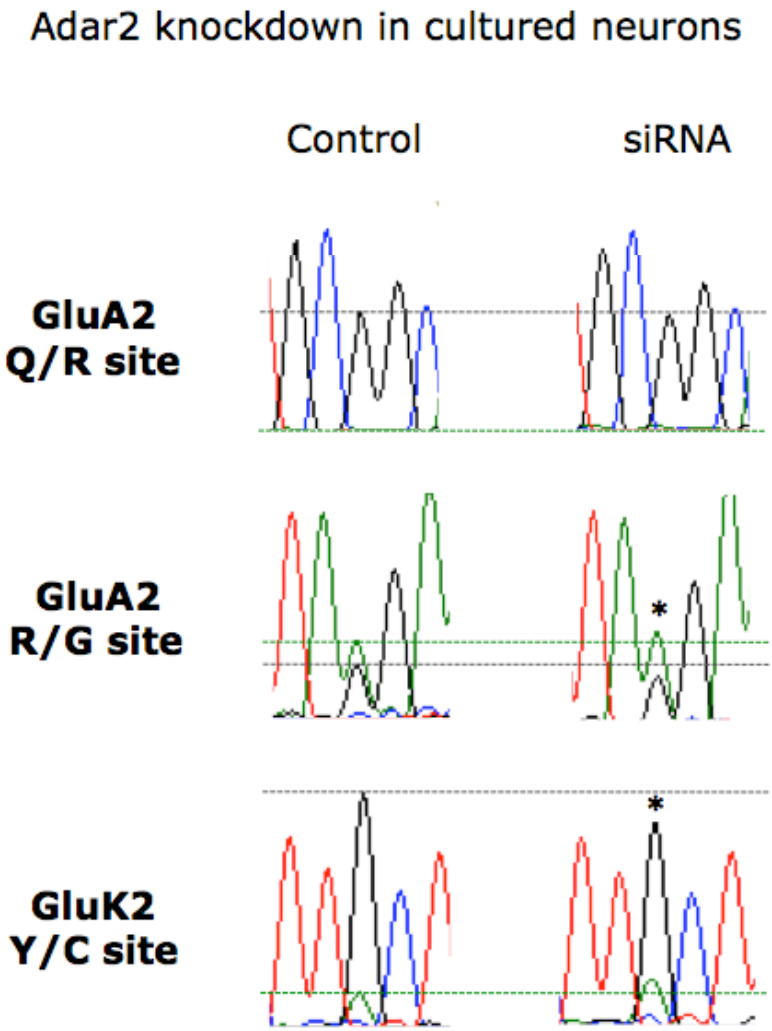

Figure S5

Modest knockdown of Adar2 in neurons does not perturb Q/R editing state of GluA2 mRNA.

Cultured hippocampal neurons were transfected with control siRNA (scrambled) and Adar2 siRNA. The GluA2 Q/R site editing status of mRNA is virtually untouched. In contrast, a decrease in A-to-I editing is apparent for the GluA2 R/G site and the Adar2 specific GluK2 Y/C site (1). The decrease in R/G editing seen here with Adar2 knock-down is quantitively similar to that observed in CA1 after chronic activity-deprivation (2). Therefore, physiological changes in editing activity are unlikely to alter the Q/R editing status of protein encoding GluA2 transcripts. Quantitatively similar results were obtained using three different siRNA sequences.

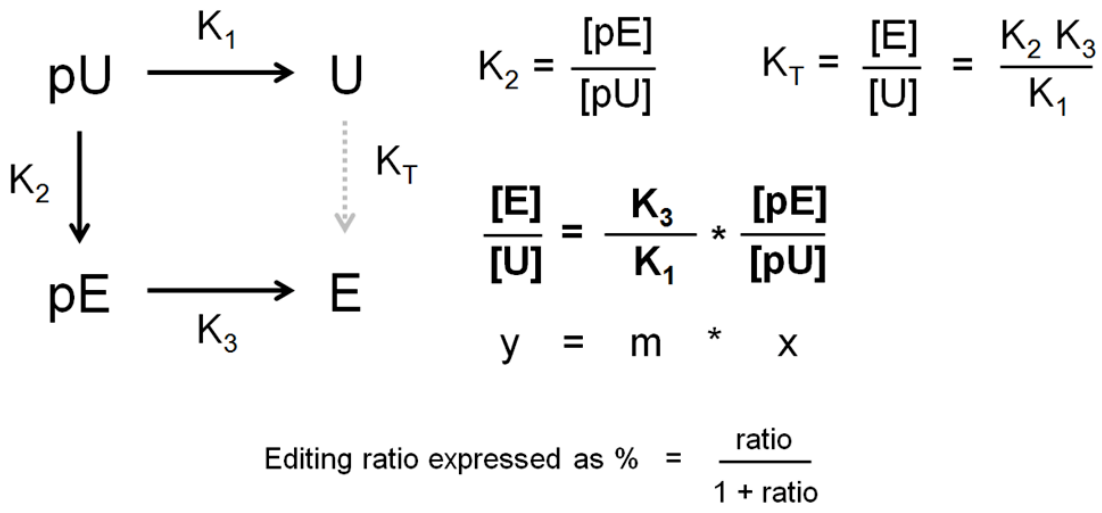

Figure S6

Reaction scheme and proof of model used to fit data in figure 5B.

In order to determine the relative splicing efficiency of edited and unedited pre-mRNAs we used the following simple model to fit our data. It can be shown that a plot of mRNA vs premRNA editing expressed as ratios will give a straight line with a slope equal to the ratio of the equilibrium constants for splicing of the edited and unedited premRNAs (K_3/K_1), which we will define here as the preferential splicing constant. When the ratios are converted to percentages the relationship between editing of mRNA vs premRNA becomes hyperbolic (see Figure 5B inset). Abbreviations: pU, pE, U and E correspond to unedited-premRNA, edited-premRNA, unedited-mRNA and edited-mRNA respectively. K_1, K_2 and K_3 are the equilibrium constants for the shown editing or splicing reaction steps. K_T is the equilibrium constant of a non-real reaction step (dashed line arrow) shown here purely for illustration purposes.

Supplemental Table 1. Details of sequence information relating to the *in silico* results presented in Figure 1

Species	Common name	Assembly / Database	Location	Coordinates	Length
Homo sapien	human	GRCh37	Chromosome 4	158257850:158258218 (+)	369
Pan troglodytes	chimpanzee	CHIMP2.1.4	Scaffold GL386479.1	3218156:3218524 (+)	369
Gorilla gorilla gorilla	gorilla	gorGor3.1	Chromosome 4	167711969:167712337 (+)	369
Pongo pygmaeus abelii	orangutan	PPYG2	Chromosome 4	163311850:163312218 (+)	369
Nomascus leucogenys	gibbon	Nleu1.0	Supercontig GL397272.1	23509395:23509763 (+)	369
Macaca mulatta	rhesus monkey	MMUL_1	Chromosome 5	149561889:149562257 (+)	369
Papio hamadryas	baboon	Pham_1.0	Scaffold Contig728022_Contig705414_Contig411886_Contig640369	92468:92836 (+)	369
Callithrix jacchus	marmoset	C_jacchus3.2.1	Chromosome 3	34907373:34907741 (-)	369
Tarsius syrichta	tarsier	tarSyr1	Scaffold scaffold_580	55489:55857 (+)	369
Otolemur garnettii	bushbaby	OtoGar3	Scaffold GL873604.1	1242599:1242967 (+)	369
Microcebus murinus	mouse lemur	micMur1	Genescaffold GeneScaffold_1453	120059:120427 (+)	369
Tupaia belangeri	treeshew	TREESHREW	Genescaffold GeneScaffold_1771	4276:4625 (+)	350
Mus musculus	mouse	GRCm38	Chromosome 3	80706568:80706937 (-)	370
Rattus norvegicus	rat	RGSC3.4	Chromosome 2	172287850:172288218 (-)	369
Cricetulus griseus	hamster	CriGri_1.0	Scaffold JH000202	1033502:1033870 (-)	369
Dipodomys ordii	kangaroo rat	dipOrd1	Genescaffold GeneScaffold_2221	66039:66407 (+)	369
Cavia porcellus	guinea pig	cavPor3	Scaffold scaffold_7	32829741:32830106 (-)	366
Ictidomys tridecemlineatus	squirrel	spetri2	Scaffold JH393386.1	3912648:3913015 (+)	368
Oryctolagus cuniculus	rabbit	oryCun2	Chromosome 15	6601066:6601434 (-)	369
Ochotona princeps	pika	Pika	Scaffold GeneScaffold_1552	81064:81431 (+)	368
Equus caballus	horse	EquCab2	Chromosome 2	76897770:76898137 (-)	369
Canis familiaris	dog	CanFam3.1	Chromosome 15	54672708:54673072 (+)	365
Felis catus	cat	Felis_catus_6.2	Chromosome B1	71345576:71345941 (-)	366
Ailuropoda melanoleuca	panda	ailMel1	Scaffold GL192663.1	633512:633907 (-)	366
Mustela putorius furo	ferret	MusPutFur1.0	Scaffold GL897066.1	4562793:4563159 (+)	367
Sorex araneus	shrew	COMMON_SHREW1	Genescaffold GeneScaffold_2352	66823:67194 (+)	372
Erinaceus europaeus	hedgehog	HEDGEHOG	Genescaffold GeneScaffold_2892	97110:97477 (+)	368
Myotis lucifugus	brown bat	Myoluc2.0	Scaffold GL429768	28118269:28118634 (-)	366
Pteropus vampyrus	fruit bat	pteVam1	Genescaffold GeneScaffold_1182	109331:109695 (+)	365
Vicugna pacos	alpaca	vicPac1	Genescaffold GeneScaffold_821	343997:344364 (+)	368
Ovis aries	sheep	OviAri1	Chromosome 17	44879716:44880083 (-)	368
Sus scrofa	pig	Sscrofa10.2	Chromosome 8	48244968:48245329 (+)	362
Bos Taurus	cow	UMD3.1	Chromosome 17	42806382:42806749 (-)	368
Loxodonta africana	elephant	loxAfr3	Supercontig scaffold_61	11317931:11318328 (-)	368
Procavia capensis	hyrax	proCap1	Genescaffold GeneScaffold_2457	63451:63817 (+)	367
Echinops telfairi	lesser hedgehog tenrec	TENREC	Genescaffold GeneScaffold_2809	163616:163984 (+)	369
Choloepus hoffmanni	sloth	choHof1	Genescaffold GeneScaffold_2629	88695:89065 (+)	371
Monodelphis domestica	opossum	BROADO5	Chromosome 5	118521108:118521471 (-)	364
Sarcophilus harrisii	tasmanian devil	DEVIL7.0	Scaffold GL864812.1	61533:61894 (-)	362
Ornithorhynchus anatinus	platypus	OANA5	Chromosome 12	14232390:14232759 (-)	370
Chrysemys picta bellii	painted turtle	ChrPicBel3.0.1	Scaffold JH584697.1	4319457:4319826 (-)	370
Pelodiscus sinensis	softshell turtle	PelSin_1.0	Scaffold JH208505.1	2227552:2227921 (+)	370
Anolis carolinensis	lizard	AnoCar2.0	Chromosome 5	128800433:128800797 (-)	365
Gallus gallus	chicken	WASHUC2	Chromosome 4	22560734:22561099 (+)	366
Meleagris gallopavo	turkey	UMD2	Chromosome 4	2053089:2053458 (+)	370
Anas platyrhynchos	duck	duck1	Scaffold scaffold456	789864:790241 (+)	378
Melopsittacus undulatus	budgerigar	MelUnd6.3	Scaffold JH556597.1	7854326:7854708 (-)	383
Taeniopygia guttata	zebra finch	taeGut3.2.4	Chromosome 4	29297181:29297566 (+)	386
Xenopus tropicalis	clawed frog	JGI_4.2	Scaffold GL172746.1	380101:380473 (+)	373
**Latimeria chalumnae*	coelacanth	LatCha1	Scaffold JH132446.1	12896:15004 (+)	2109
**Lepisosteus oculatus*	gar	LepOcu1	Chromosome LG4	20861481:20861882 (-)	402
Callorhinchus milii	shark	Eshark 1.4X	WGS AAVX01041233.1	1724:2145 (-)	422

All sequence data was obtained via Ensembl (http://www.ensembl.org, accessed 05/08/2012) except shark sequence, which was from the IMBC elephant shark genome project: http://esharkgenome.imcb.a-star.edu.sg/. *Data from marked species were used only in Figure 1C for sequence comparison of Q/R site editing substrate. Nonetheless their inclusion in the alignment would give a similar secondary structure and results as that shown in Figure 1A and B.

Supplemental Table 2. Sequences of morpholino oligonucleotides used in this study. Small bold letters indicate the sequence at mismatch positions.

Antisense	5′- ATG AGA ATA TGC AGC AAA AAC ACG G -3′
Control	5′- CCT CTT ACC TCA GTT ACA ATT TAT A -3′
Invert	5′- GGC ACA AAA ACG ACG TAT AAG AGT A -3′
Mismatch	5′- ATG A**c**A ATA T**c**C **t**G**g** AAA AA**g** ACG G -3′

Supplemental Table 3. Comparison of % editing between region CA1 microdissected from organotypic hippocampal slice and the cell lines used in this study for some A-to-I editing sites in GluA2.

	Hippocampal CA1	**SH-SY5Y**	**MIN-6**
pre-mRNA			
Q/R	95	24	100
Hotspot 1			
+60	54	8	35
Hotspot 2			
+262	20	27	60
+263	46	5	59
+264	8	1	24
R/G	33	n.d	n.d
mRNA			
Q/R	100	84	100
R/G	31	n.d.	75

Note the extent of editing at these sites in MIN-6 is more like that observed in whole brain extract (see (1). n.d. not determined. SH-SY5Y and MIN-6 are cell lines with low and high A-to-I editing activity respectively.

Supplemental References

1. Higuchi, M., Maas, S., Single, F.N., Hartner, J., Rozov, A., Burnashev, N., Feldmeyer, D., Sprengel, R. and Seeburg, P.H. (2000) Point mutation in an AMPA receptor gene rescues lethality in mice deficient in the RNA-editing enzyme ADAR2. *Nature*, **406**, 78-81.
2. Penn, A.C., Balik, A., Wozny, C., Cais, O. and Greger, I.H. (2012) Activity-mediated AMPA receptor remodeling, driven by alternative splicing in the ligand-binding domain. *Neuron*, **in press**.